Collagen V is a dominant regulator of collagen fibrillogenesis: dysfunctional regulation of structure and function in a corneal-stroma-specific *Col5a1*-null mouse model

Mei Sun[1], Shoujun Chen[1], Sheila M. Adams[1], Jane B. Florer[2], Hongshan Liu[3], Winston W.-Y. Kao[3], Richard J. Wenstrup[4] and David E. Birk[1,*]

[1]Department of Pathology and Cell Biology, University of South Florida College of Medicine, 12901 Bruce B. Downs Blvd, Tampa, FL 33612, USA
[2]Department of Human Genetics, Cincinnati Children's Hospital Research Foundation, Cincinnati, OH 45229, USA
[3]University of Cincinnati, Department of Ophthalmology, 3230 Eden Ave, Cincinnati, OH 45267, USA
[4]Myriad Genetic Laboratories, Inc., Salt Lake City, UT 84108, USA
*Author for correspondence (dbirk@health.usf.edu)

Accepted 7 July 2011
Journal of Cell Science 124, 4096–4105

doi: 10.1242/jcs.091363

Summary

Collagen V is a regulatory fibril-forming collagen that forms heterotypic fibrils with collagen I. Deletion of collagen V in the mouse is associated with a lack of fibril assembly in the embryonic mesenchyme, with a resultant lethal phenotype. The current work elucidates the regulatory roles of collagen V during development and growth of tissues. A conditional mouse model with a mutation in *Col5a1* was developed using a Cre-*loxP* approach. *Col5a1* was ablated in $Col5a1^{flox/flox}$ mice using a cornea stroma-specific *Kera*-Cre driver mouse to produce a bitransgenic $Col5a1^{\Delta st/\Delta st}$ line that is null for collagen V. This permits analyses of the corneal stroma, a widely used model for studies of collagen V. The collagen-V-knockout stroma demonstrated severe dysfunctional regulation of fibrillogenesis. Fibril diameters were significantly increased, with an abnormal, heterogeneous distribution; fibril structure was abnormal, fibril number was decreased and lamellae were disorganized with decreased stroma thickness. The phenotype was more severe in the anterior versus posterior stroma. Opacity was demonstrated throughout the $Col5a1^{\Delta st/\Delta st}$ stroma, with significantly increased haze intensity compared with control mice. These data indicate central regulatory roles for collagen V in fibril and matrix assembly during tissue development, with dysfunctional regulation resulting in a functional loss of transparency.

Key words: Collagen V, Cornea, Fibrillogenesis, Stroma, Extracellular matrix, Collagen-V-knockout mouse

Introduction

Collagen V is a member of a subclass of fibril-forming collagens that retain portions of the N-terminal peptide domain. It is involved in the regulation of fibril assembly and can be classified as a regulatory fibril-forming collagen (Birk and Bruckner, 2011). The major isoform of collagen V, $[\alpha1(V)]_2\alpha2(V)$, co-assembles with collagen I to form heterotypic fibrils (Birk et al., 1988). Collagen V is a quantitatively minor component relative to collagen I, comprising 2–5% of the total collagen in most tissues, e.g. dermis, tendon and bone, but in the cornea, it constitutes 10–20% (Birk, 2001; Segev et al., 2006). Much of the elucidation of collagen I and V heterotypic fibril structure and analysis of its regulatory interactions have been done in the corneal stroma (Birk et al., 1988; Birk, 2001; Linsenmayer et al., 1993; Marchant et al., 1996). The stroma contains a homogeneous population of small-diameter fibrils with regular packing, organized as orthogonal lamellae. This ordered structure results in minimal light scattering and optical transparency (Hassell and Birk, 2010). The tightly controlled assembly of stromal structure and function makes it an ideal model for elucidating the mechanisms regulating tissue-specific collagen fibrillogenesis and matrix assembly.

A collagen-V-knockout mouse model homozygous for a targeted deletion in the *Col5a1* gene was embryonic lethal, and did not develop past the onset of organogenesis (Wenstrup et al., 2004a). In the embryonic mesenchyme, few fibrils were assembled in the absence of collagen V and presence of normal amounts of collagen I. These data indicate a critical role for collagen V in the nucleation of fibril assembly in the low collagen concentration environment of the embryonic mesenchyme. This critical role is consistent with the embryonic lethality of *Co5a1* ablation and provides an explanation for why patients homozygous for mutations that do not produce collagen V alpha 1 chains have not been described, whereas haplo-insufficiency in *COL5A1* is common (Schwarze et al., 2000; Wenstrup et al., 2000). However, it is well known that collagen I can self-assemble into fibrils in vitro in the absence of collagen V. Fibrils with normal D-periodic cross-striations are assembled indicating that nucleators, such as collagen V, are not required when collagen concentrations are above relatively high critical levels. Collagen V has been shown to nucleate collagen fibril formation in self-assembly assays in vitro, in cell culture studies and in mouse models (Birk et al., 1990; Birk, 2001; Marchant et al., 1996; Wenstrup et al., 2004a; Wenstrup et al., 2004b).

Journal of Cell Science

The nucleation of fibril formation by collagen V provides a mechanism whereby the fibroblast can regulate fibril diameter in a tissue-specific manner by regulating the ratio of nucleators to a given collagen concentration. For instance, collagen V is a larger percentage of the total fibril-forming collagen in the corneal stroma than in dermis and tendon. The large number of nucleation sites in the cornea would contribute to the formation of small-diameter fibrils necessary for transparency, whereas the lower number in the tendon and the dermis leads to larger-diameter fibrils required for mechanical strength. In addition, the fibroblast can define the site of nucleation and control fibril organization.

The classic form of Ehlers–Danlos syndrome (EDS, types I/II) is a generalized connective tissue disorder with broad tissue involvement characterized by fragile, hyperextensible skin, widened atrophic scars, joint laxity, a high prevalence of aortic root dilation and other manifestations of connective tissue weakness (Beighton, 1992; Beighton et al., 1998; Malfait et al., 2010; Steinmann et al., 2002). The most common reported molecular mechanism in classic EDS is the functional loss of one *COL5A1* allele (Schwarze et al., 2000; Wenstrup et al., 2000), with a haplo-insufficiency for collagen V. Abnormal fibril formation is seen in the classic EDS and the dermis of EDS patients contains large, irregular collagen fibrils (Hausser and Anton-Lamprecht, 1994; Vogel et al., 1979). Studies using fibroblasts from EDS patients with characterized mutations in *COL5A1* and a mouse *Col5a1*$^{+/-}$ model of classic EDS have demonstrated that heterotypic collagen I and V interactions are involved in the regulation of fibril diameter and fibril number (Segev et al., 2006; Wenstrup et al., 2004a; Wenstrup et al., 2004b; Wenstrup et al., 2006). The *Col5a1* heterozygous mice are haplo-insufficient and have a phenotype comparable to that of classic EDS (Wenstrup et al., 2006). In the dermis, there were two populations of fibrils, a structurally aberrant one and one with normal fibril structure, but larger fibril diameters. In addition, there were fewer fibrils assembled than in wild-type controls. This suggested a concentration-limited nucleation of fibril assembly, with the abnormal fibrils resulting from unregulated assembly. In the corneas of these mice, all fibrils had normal structure, but with larger diameters than the wild-type controls. This indicated that in the high collagen V concentration cornea, collagen V did not become limiting. However, there were fewer nucleation events due to the reduced level of collagen V, with collagen I concentration comparable to that in the control, resulting in a single population of larger fibrils. These data suggest a role for collagen V in nucleation of fibril assembly.

The purpose of this investigation is to elucidate the role of collagen V in the regulation of corneal stromal fibrillogenesis. A conditional mouse model with a null mutation in *Col5a1* targeted to the corneal stroma was generated using a Cre-*loxP* approach. This approach permits the study of the regulation of fibrillogenesis in the high collagen concentration environment of growing and mature tissues by avoiding the embryonic lethal phenotype encountered in the conventional gene deletion mouse model. The results demonstrate that the absence of collagen V results in dysfunctional nucleation and fibril assembly. This leads to a severe disruption in corneal fibrillogenesis, matrix assembly and function, defining a critical role for collagen V in the regulation of fibrillogenesis and development of a functional cornea.

Results

Creation of a conditional collagen-V-knockout mouse model

To elucidate the functional roles of collagen V in the regulation of collagen fibrillogenesis, a conditional mouse line was created. Homozygous null mice carrying a standard targeted deletion of *Col5a1* exhibit an embryonic lethal phenotype (Wenstrup et al., 2004a). To overcome this limitation, a cornea-stroma-specific *Col5a1*-null mouse line was generated using a Cre-*loxP*-mediated

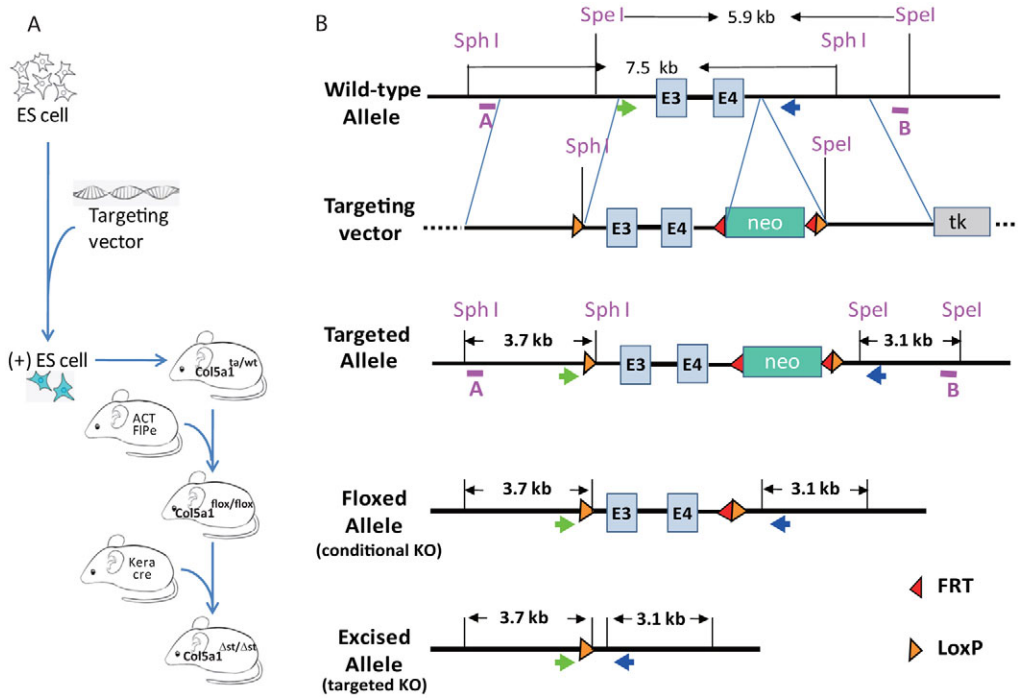

Fig. 1. Strategy for the creation of cornea-specific *Col5a1* conditional-knockout mice. (**A**) Strategy for gene targeting of embryonic stem cells and generation of stroma-specific *Col5a1* conditional-knockout mice. (**B**) Schematic diagram of wild-type *Col5a1*, targeting construct, targeted allele, floxed allele and excised allele after Cre recombination of *Col5a1* gene. *Spe*I and *Sph*I sites were used to insert the loxP sequence and Neo cassette. The Neo cassette was flanked by two FRT sites. The purple bars show the location of probe A and B, which were used in the Southern blot analysis to screen the targeted ES cells. The colored arrows indicate the location of the primers used to confirm the excision in *Col5a1* by Cre recombination.

conditional gene-knockout approach (Fig. 1). The alpha 1 chain of collagen V was targeted because all collagen V isoforms contain this chain. The strategy was to flank exons 3 and 4 in the *Col5a1* gene with loxP elements. Cre excision would result in a nonsense mutation with a premature stop codon. The excision of *Col5a1* exon 3 and 4 generated a premature stop codon, thus truncated the synthesis of collagen V. Only a small, non-functional peptide can be potentially translated. This putative small peptide contains the signal peptide and a portion of the non-collagenous domain 3 (NC3). The truncated collagen V peptide would be unable to form a stable triple helix. In addition, the chain selection domain is absent. A similar deletion strategy was used in the standard targeted deletion (Wenstrup et al., 2004a). Cre was targeted to the corneal stromal keratocytes by crossbreeding *Kera*-Cre mice with $Col5a1^{flox/flox}$ mice thus creating bitransgenic mice where Cre expression is targeted to the corneal keratocytes using the keratocan promoter sequence. This resulted in a targeted deletion of *Col5a1* in the corneal stroma in $Col5a1^{\Delta st/\Delta st}$ mice. Unlike the mid-gestation lethality of conventional collagen-V-knockout mice, $Col5a1^{\Delta st/\Delta st}$ mice were viable and fertile. There was no significant difference in the body weight between wild-type mice and $Col5a1^{\Delta st/\Delta st}$ mice at post-natal day (P)10 and P30 (data not shown).

Characterization of conditional collagen-V-knockout mouse model

As expected, floxed *Col5a1* alleles were identified in genomic DNA isolated from tails of $Col5a1^{flox/flox}$ and $Col5a1^{\Delta st/\Delta st}$, but not wild-type mice, using PCR analysis. A 150 bp PCR product was amplified from tail DNA in the wild-type mice, and a 272 bp PCR product from the floxed allele in the $Col5a1^{flox/flox}$ and $Col5a1^{\Delta st/\Delta st}$ mice. In addition, the expression of the *Kera*-Cre transgene was characterized. A Cre PCR product was amplified only in the bitransgenic $Col5a1^{\Delta st/\Delta st}$ mice and not in the $Col5a1^{flox/flox}$ or wild-type mice. These data indicate that the $Col5a1^{\Delta st/\Delta st}$ mice contain the floxed *Col5a1* alleles and express Cre (Fig. 2A). The tissue specificity of the *Kera-Cre* recombinase activity was determined by breeding a male mT/mG double reporter mouse with female *Kera*-Cre mice (Fig. 2B). Analysis of the offspring demonstrated corneal-stroma-specific Cre excision. To analyze the targeting of Cre double reporter mice were used. Stromal keratocytes expressed mEGFP resulting from Cre recombinase activity. However, the corneal epithelium and endothelium expressed the red fluorescence, indicating a lack of excision. There was no Cre recombinase activity in muscle and other tissues in the eye, including sclera and iris. These data demonstrate a specific targeting of Cre recombinase to the corneal stroma keratocytes using the *Kera*-Cre 4.2 mice.

The excision of exons 3 and 4 in the $Col5a1^{flox/flox}$ by Cre-recombinase in the corneal stroma of $Col5a1^{\Delta st/\Delta st}$ mice was demonstrated using qualitative PCR of corneal stroma DNA as a template (Fig. 2C). A pair of PCR primers located upstream of exon 3 and downstream of exon 4 was designed and a 391 bp PCR product was amplified from $Col5a1^{\Delta st/\Delta st}$ corneal stroma DNA. By contrast, a large PCR product that included exons 3 and 4 (over 2500 bp) was amplified in the $Col5a1^{flox/flox}$ and wild-type mice. These data demonstrate the targeted deletions of exons 3 and 4 in the corneal stroma of $Col5a1^{\Delta st/\Delta st}$ mice.

Null expression of *Col5a1* after *Kera*-Cre-mediated excision of exons 3 and 4 was confirmed using Real Time PCR (Fig. 2D). *Col5a1* mRNA expression was decreased to near baseline in the

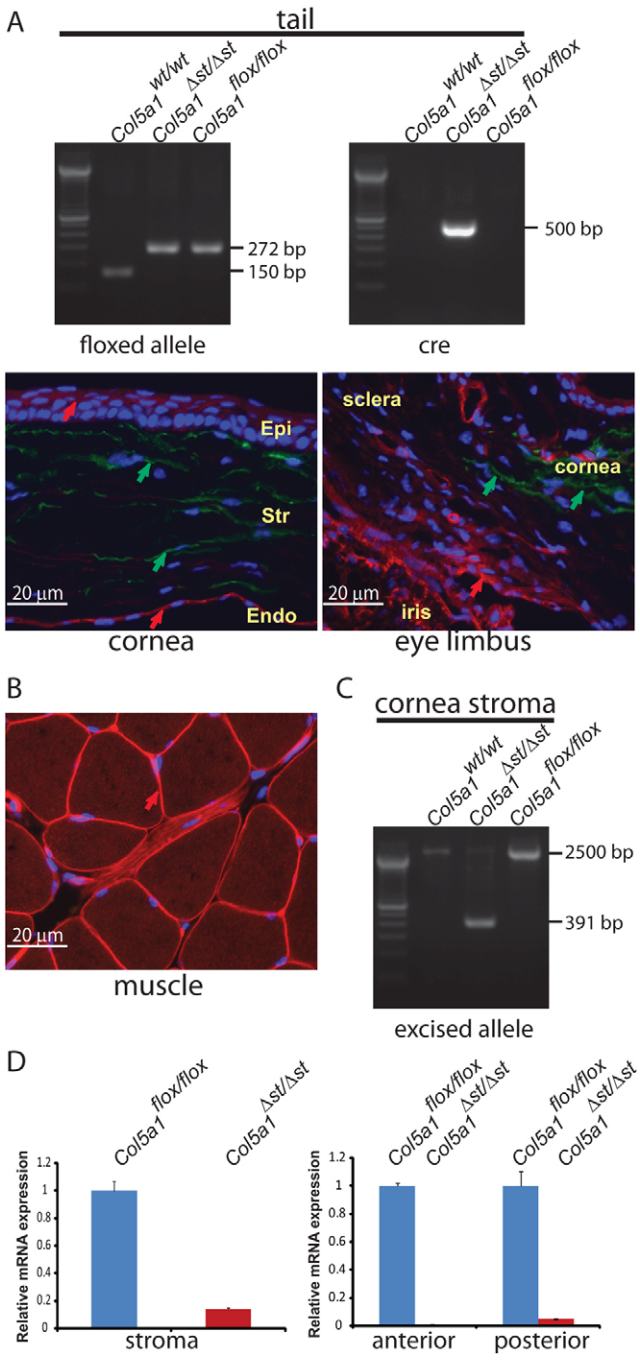

Fig. 2. Targeted deletion of *Col5a1* in the cornea stroma of $Col5a1^{\Delta st/\Delta st}$ mice. (**A**) PCR genotyping analysis of tail tissue from *Col5a1* conditional-knockout mice. $Col5a1^{wt/wt}$, wild-type mice; $Col5a1^{flox/flox}$, *Col5a1* conditional-knockout mice with homozygous floxed alleles; $Col5a1^{\Delta st/\Delta st}$, stroma-specific *Col5a1*-null mice. (**B**) *Kera*-Cre excision was targeted to the corneal stroma. Expression of the red colored membrane-targeted tandem dimer Tomato Red (Mt) was observed in keratocytes before Cre-mediated excision (red arrows) and the membrane-targeted green fluorescent protein (mG) in keratocytes after excision (green arrows). Fluorescence microscopy of the central cornea, limbus and skeletal muscle from P30 offspring of *Kera*-Cre and mT/mG matings. (**C**) A tissue-specific Cre excision of an allele in $Col5a1^{\Delta st/\Delta st}$ mice cornea stroma demonstrated by PCR. (**D**) Real-time PCR analysis shows a decrease of *Col5a1* mRNA expression by 92% in $Col5a1^{\Delta st/\Delta st}$ corneal stroma. (**E**) *Col5a1* mRNA expression analyzed in the anterior and posterior stroma using laser-capture microdissection.

Col5a1$^{\Delta st/\Delta st}$ corneal stroma compared with control samples. This indicated a null genotype in the *Col5a1*$^{\Delta st/\Delta st}$ corneal stroma. Previous reports have indicated anterior and posterior differences in corneal structure, and severity of mutant phenotypes in mouse models (Chen et al., 2010; Zhang et al., 2009). Therefore, collagen V expression in the anterior and posterior stroma was analyzed. Samples from the anterior and posterior stroma were isolated using laser capture micro-dissection and a qPCR analysis was performed. The expression of *Col5a1* mRNA was completely abolished in the *Col5a1*$^{\Delta st/\Delta st}$ anterior corneal stroma and was at or near baseline in the posterior stroma (Fig. 2D). These data indicate that the *Col5a1*$^{\Delta st/\Delta st}$ corneal stroma is null for collagen V expression.

Col5a1$^{\Delta st/\Delta st}$ mice do not express collagen V in the corneal stroma

Analysis of collagen V in the corneal stroma was performed using immunoblots and immunofluorescence localization (Fig. 3). The α1(V) chain of collagen V was not detectable in the cornea from *Col5a1*$^{\Delta st/\Delta st}$ adult mice (Fig. 3A,B), consistent with the mRNA data. By contrast, the α2(V) chain expression was decreased and the α1(I) chain of collagen I demonstrated comparable expression in *Col5a1*$^{\Delta st/\Delta st}$ and control corneas (Fig. 3A). Reactivity against collagen V was homogeneously localized throughout the wild-type stroma by immunofluorescence microscopy. However, there was a virtual absence of collagen V reactivity in the *Col5a1*$^{\Delta st/\Delta st}$ corneal stroma (Fig. 3C). The data indicate that no collagen V is expressed in the corneal stroma of *Col5a1*$^{\Delta st/\Delta st}$ mice. By contrast, the

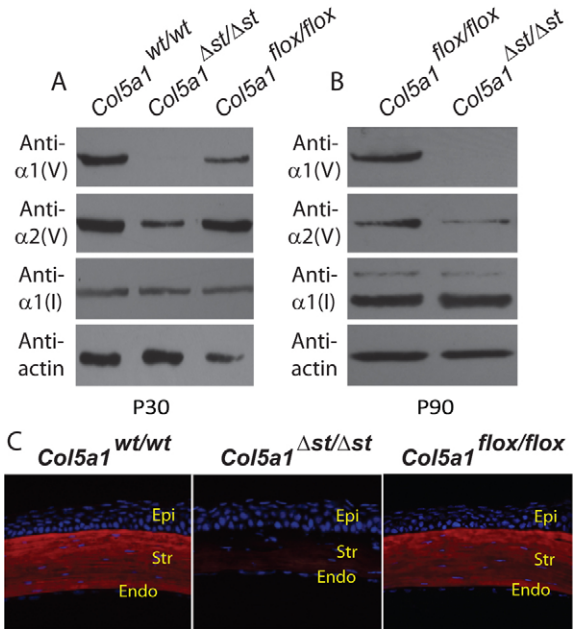

Fig. 3. The corneal stroma of the *Col5a1*$^{\Delta st/\Delta st}$ mouse is null for collagen V. (**A**) The expression of α1 chain of collagen V in the *Col5a1*$^{\Delta st/\Delta st}$ mouse cornea at P30 is absent whereas the expression of α2 chain of collagen V decreases and α1 chain of collagen I does not change compared with wild-type and *Col5a1*$^{flox/flox}$ control mice. (**B**) Collagen V is absent in the *Col5a1*$^{\Delta st/\Delta st}$ mouse cornea at age P90 by western blot analysis. (**C**) Absence of collagen V in the stromal-specific *Col5a1*$^{\Delta st/\Delta st}$ mouse. Localization of collagen V (red) in P30 mouse cornea from wild type, *Col5a1*$^{flox/flox}$ control and *Col5a1*$^{\Delta st/\Delta st}$ is shown using immunofluorescence microscopy. Nuclear localization was shown using DAPI (blue).

Col5a1$^{flox/flox}$ mice expressed the α1(V) chain of collagen V at a level comparable to that in wild-type mice, indicating that the genetic manipulation and insertion of loxP elements did not alter the function of the *Col5a1* gene.

Aberrant fibril structure and corneal stromal organization in the absence of collagen V

Grossly, adult *Col5a1*$^{\Delta st/\Delta st}$ mice displayed conspicuous corneal stromal opacity (Fig. 4A). Structurally, the corneal opacity is associated with abnormal fibril structure and stromal disorganization (Fig. 4B,C). In mature (P30) wild-type control mice, collagen fibrils had small, homogeneous diameters when analyzed using transmission electron microscopy. The fibrils were regularly packed and formed well-organized, interwoven lamellae. However, the mature *Col5a1*$^{\Delta st/\Delta st}$ stroma was composed of collagen fibrils with a heterogeneous fibril population containing fibrils with very large diameters. Structurally aberrant fibrils with irregular profiles were common. In addition, the fibrils were irregularly packed and lamellar organization was disrupted. This phenotype was comparable in P30 and P90 *Col5a1*$^{\Delta st/\Delta st}$ mice.

Altered corneal fibrillogenesis in the absence of collagen V

A striking disruption in fibril structure in the *Col5a1*-null mouse cornea was demonstrated in ultrastructural analyses of the stroma. Compared with wild-type control mice, *Col5a1*$^{\Delta st/\Delta st}$ mice displayed larger and less uniformed collagen fibrils throughout the cornea stroma, with disrupted fibril packing. However, there was an anterior–posterior difference in the fibril phenotype, with the anterior stroma containing larger and more heterogeneous fibrils than the posterior stroma (Fig. 5A). An analysis of fibril diameter distributions demonstrated significant differences in fibril structure between *Col5a1*$^{\Delta st/\Delta st}$ and control corneas (Fig. 5B). In the anterior stroma, the mean stromal fibril diameter increased from 25.3±3.4 nm in the control corneas to 42.5±12.8 nm in the *Col5a1*$^{\Delta st/\Delta st}$ corneas. The mean diameter of the fibrils in the posterior stroma increased to 34.7±6.7 nm in the *Col5a1*$^{\Delta st/\Delta st}$ mice, compared with 27.5±3.3 nm in the control mice. Differences in both the anterior and posterior regions were statistically significant ($P<0.0001$). In addition to the shift to larger diameter fibrils in the *Col5a1*$^{\Delta st/\Delta st}$ corneas, there was a substantial broadening of the diameter distribution compared with controls, indicating a more heterogeneous fibril population. Both the anterior and posterior *Col5a1*-null stroma had a population of fibril diameters with a normal distribution. However the range was 8–95 nm in the anterior stroma compared with 12–61 nm in the posterior stroma. In comparison, the range of fibril diameters in the anterior and posterior stroma from control corneas was 14–42 nm and 14–39 nm, respectively. Associated with the alterations in fibril structure, the *Col5a1*$^{\Delta st/\Delta st}$ corneas contained fewer fibrils than in the control corneas. In both anterior and posterior regions of the stroma, there was a decrease in fibril density in the *Col5a1*-null stromas compared with the controls (Fig. 5C). A significant ($P<0.0001$) decrease in the number of fibrils per unit area (μm^2) of 58% in the anterior stroma and 36% in the posterior stroma of *Col5a1*$^{\Delta st/\Delta st}$ compared with control corneas was observed. This is representative of a decrease in the number of fibrils assembled in the *Col5a1*-null stroma. The decreased fibril density and larger-diameter fibrils in the *Col5a1*$^{\Delta st/\Delta st}$ stromas were associated with a decrease in the inter-fibrillar space compared with that in control

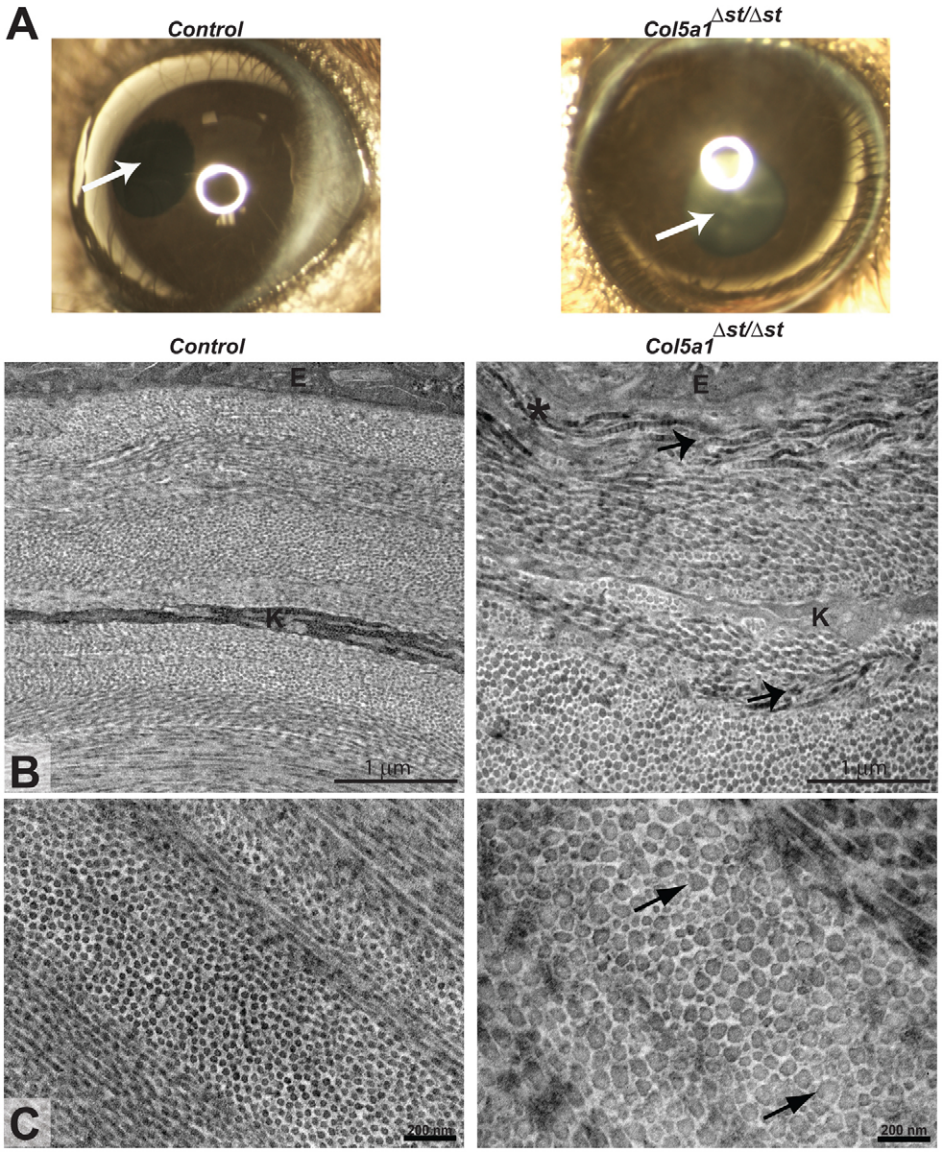

Fig. 4. Stromal structure and function is disrupted in the absence of collagen V. (**A**) Corneal opacity is observed in mature (P60) *Col5a1*$^{\Delta st/\Delta st}$ mice. (**B**) Transmission electron micrographs of cornea anterior stroma show the regular packing of the lamellae in wild-type control mouse and the disorganized lamellae packing in *Col5a1*$^{\Delta st/\Delta st}$ corneas. This is associated with very large fibrils with abnormal structures (arrow). The epithelial basement membrane is also interrupted in the *Col5a1*$^{\Delta st/\Delta st}$ mouse cornea (asterisk). (**C**) Higher-magnification transmission electron micrographs show fewer, and abnormally large-diameter fibrils with aberrant structures (arrow) in the *Col5a1*-null mouse stroma compared with the controls. E, epithelial cell; K, keratocyte.

stromas (Fig. 5D). The decrease in inter-fibril space was significant in the anterior stroma ($P<0.01$) as well as the posterior stroma ($P<0.05$).

Disruption of stromal architecture in *Col5a1*$^{\Delta st/\Delta st}$ mice

Corneal stromal architecture was assessed using non-linear optical imaging of second harmonic generated signals (SHG) (Fig. 6). The SHG signals can be used to access lamellar organization in the cornea (Morishige et al., 2006). The SHG signals are dependent on intrinsic order in tissues such as that derived from organized collagen fibrils in the corneal stroma (Han et al., 2005). Forward-scattered signals result from the collagen fibrils. The forward-scattered SHG signals showed similar small bands of interwoven lamellae with a uniform distribution in the anterior (Fig. 6A) and posterior stroma (data not shown) in the control mouse cornea. In comparison, in the *Col5a1*-null stromas of *Col5a1*$^{\Delta st/\Delta st}$ mice, much larger bands of uneven fibers were observed, especially in anterior stroma. This is consistent with larger fibrils with a higher density packing of fibrils within lamellae. Backward-scattered SHG signals are sensitive to the order of fibrils, with order associated with low signal, and disorder associated with intense signal. Intense backscattered SHG signals were obtained in the *Col5a1*-null stroma, with signals generated by disorganized collagen-containing lamellae (Fig. 6B). By contrast, the control stroma had a low-intensity backscattered SHG signal, which is consistent with well-ordered stromal lamellae. These data demonstrate that disruption of fibril assembly and organization significantly impacted higher order lamellar structure with lamellar architecture being less ordered in the absence of collagen V.

Dysfunctional regulation of fibrillogenesis results in decreased cornea stromal thickness and cornea transparency

A non-invasive analysis of corneal light scattering and stromal thickness was done using in vivo confocal microscopy. Grossly, the *Col5a1*$^{\Delta st/\Delta st}$ mice exhibited cloudy corneas (Fig. 4A). Corneal opacity was analyzed in *Col5a1*$^{\Delta st/\Delta st}$ and control mice at P60 (Fig. 7A). In *Col5a1*$^{\Delta st/\Delta st}$ mice, backscattered light was observed throughout the corneal stroma. However, there was an

anterior–posterior difference, with more haze in the anterior stromas. By contrast, the control stroma demonstrated little scattered light. Both control and *Col5a1*$^{\Delta st/\Delta st}$ mice demonstrated scattered light at the epithelial surface as a result of reflection at this interface. A three-dimensional image was rendered from the corneal epithelium to the endothelium (Fig. 7B). The epithelium and endothelium from *Col5a1*$^{\Delta st/\Delta st}$ and control mice were comparable in cell number and thickness. However, a significant decrease ($P<0.05$) in stromal thickness was observed in *Col5a1*$^{\Delta st/\Delta st}$ compared with wild-type mice (Fig. 7C). This decrease of 14% is consistent with the differences observed in the immunostaining analyses (Fig. 3C). Scattered light in the stroma was quantitatively assessed (Fig. 7D). There was increased backscattered light in the anterior versus the posterior stroma, consistent with the structural phenotype; however, in both regions, backscatter was considerably greater than in the control stroma. Total pixel intensity of the three-dimensional volume was divided by stromal thickness and the average light scattering per micrometer thickness of the corneal stroma was calculated. In the *Col5a1*$^{\Delta st/\Delta st}$ mice, the light scattering was 3.5-fold greater than in control mice. The observed difference was statistically significant ($P<0.01$).

In summary, a conditional knockout of *Col5a1* was created and targeted to the corneal stroma. This resulted in a *Col5a1*-null stroma with no alteration in collagen I. The *Col5a1*$^{\Delta st/\Delta st}$ mice had grossly cloudy corneas associated with scattered light in the stroma. This functional defect was associated with a dysfunctional regulation of fibril assembly. In the absence of collagen V, a broad heterogeneous population of fibrils was assembled with abnormal structures. The fibrils were poorly organized and lamellar architecture was disrupted. Collagen fibrillogenesis is tightly regulated and disruption at any of these levels is inconsistent with corneal transparency. In addition, fewer fibrils were assembled, and there was a decrease in stromal thickness. These data demonstrate key regulatory roles for collagen V in: (1) nucleation, where it determines the number of fibrils initiated; (2) initial fibril assembly, where it regulates fibril structure, i.e. diameter and circular cross-sectional profiles; and (3) fibril packing and regular orthogonal organization of lamellae. Regulation of these key steps is central to the normal development of corneal structure and function.

Discussion

In the current study, we demonstrated collagen V as a central regulator of collagen fibril formation, matrix assembly and tissue function in the corneal stroma. In the absence of collagen V,

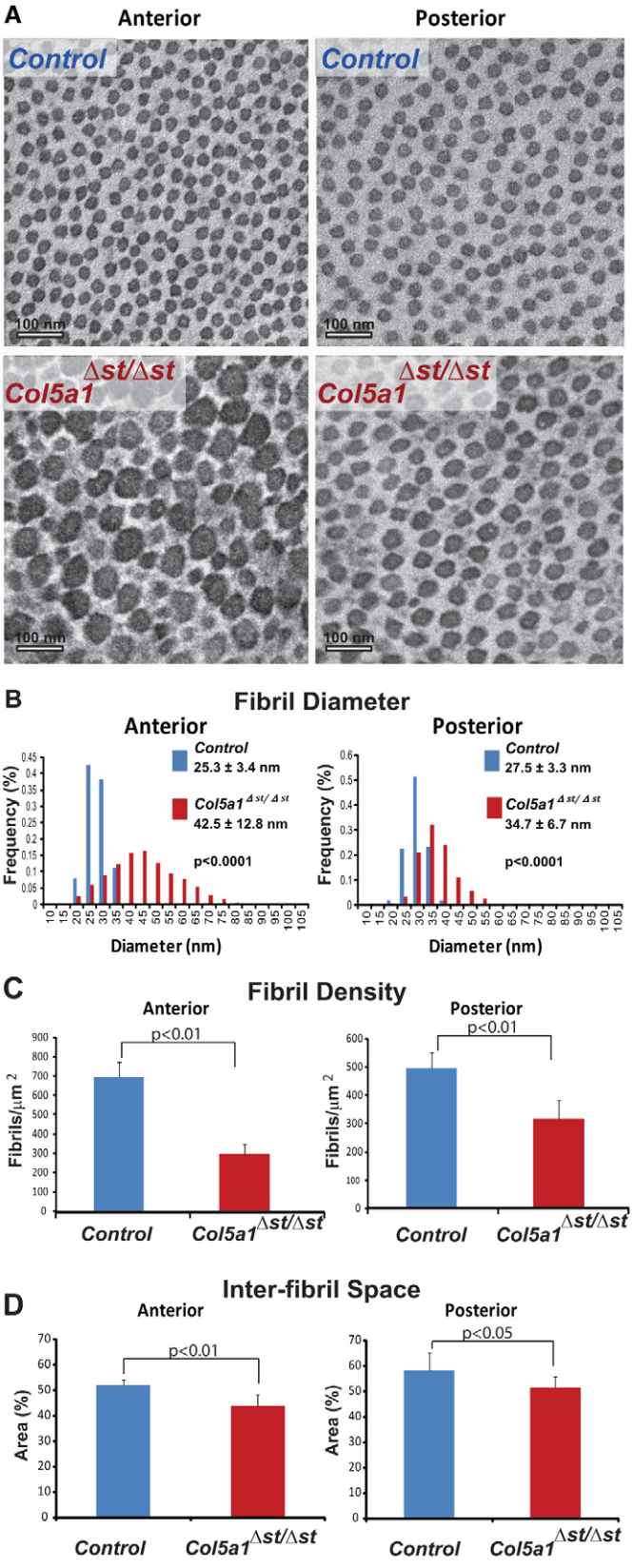

Fig. 5. Abnormal fibril structure in the stroma of *Col5a1*$^{\Delta st/\Delta st}$ P30 mice. (**A**) Transmission electron micrographs of the anterior and posterior stroma from wild-type and *Col5a1*$^{\Delta st/\Delta st}$ corneal stromas. Scale bar: 100 nm. (**B**) Histograms present the distribution of fibril diameters in the anterior and posterior stroma of control and *Col5a1*$^{\Delta st/\Delta st}$ mice. Fibril diameters increase with a broader distribution throughout the anterior and posterior stroma in *Col5a1*$^{\Delta st/\Delta st}$ mice compared with control mice. However, the abnormal fibril phenotype is more severe in the anterior stroma. In the anterior stroma, the range of diameters in control mice is 13.7–41.8 nm versus 7.7–95.0 nm in the *Col5a1*$^{\Delta st/\Delta st}$ mice, compared with 13.7–38.8 nm and 11.3–60.9 nm, respectively, in the posterior stroma. (**C**) Fibril density analysis shows a significant decrease in fibril number in both the anterior and posterior stroma of *Col5a1*$^{\Delta st/\Delta st}$ mice compared with wild-type mice. (**D**) Inter-fibril space in anterior and posterior stroma is also decreased in *Col5a1*$^{\Delta st/\Delta st}$ mice. Measurements were collected from three different mice from each group; four electron micrograph images of non-overlapping areas of both the anterior and posterior stroma were acquired from each mouse. The error bars (± s.d) and Student's *t*-test were obtained from analysis of 12 images.

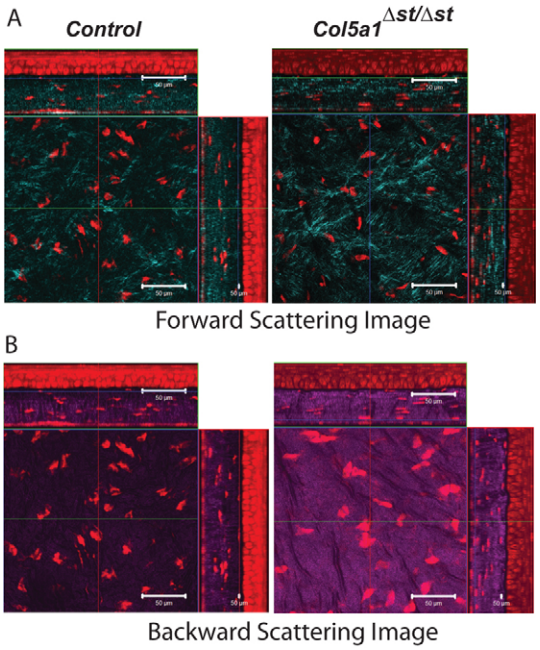

Fig. 6. *Col5a1*-null corneal stromas have disorganized stromal architecture. (**A**) The SHG forward-scattering images show larger and interwoven fibers (cyan) in the *Col5a1*-null stroma. The fibers in the control mouse are smaller and better organized. (**B**) The back-scattering images show more flattened and more transparent images in the control mouse whereas the lamellae (magenta) in the conditional-knockout mouse are disorganized and have grooves into the deeper stroma. The corneas are also stained with Syto 59 (Red) to reveal the nucleus of the keratocytes under confocal fluorescence microscope. Scale bars: 50 μm.

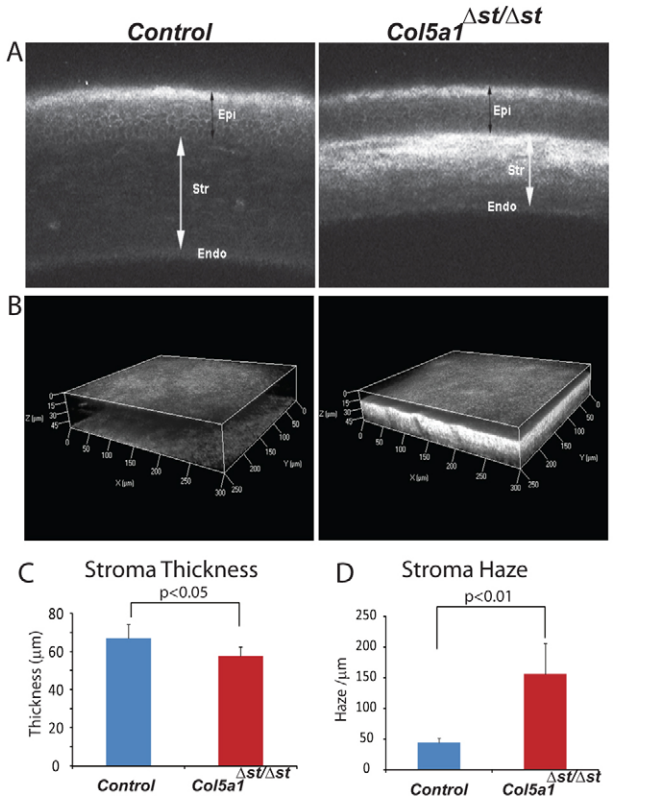

Fig. 7. Corneal stromal transparency is greatly decreased in stroma-specific knockout mouse. (**A**) In vivo confocal microscopy images taken in the *x*–*z* planes of the corneal cross-section show a decrease in the thickness of the stroma, but not the epithelium. Epi, epithelium; Str, stroma; Endo, endothelium. (**B**) Rendered 3D images of HRT examination reveal a clear and transparent cornea with little backscattered light in the control mouse and significant increase in light scattering and a decrease in the cornea thickness in the $Col5a1^{\Delta st/\Delta st}$ mice (**C**) The cornea stroma thickness is decreased in the $Col5a1^{\Delta st/\Delta st}$ mice (n=6; P<0.05). (**D**) The average pixel intensity per mm of light scattering in the whole corneal stroma is significantly increased in $Col5a1^{\Delta st/\Delta st}$ mice (n=6; P<0.01). Results are mean ± s.d.

fewer fibrils were assembled, fibrils had altered structures and fibril organization, as well as tissue architecture, was disrupted. Abnormal regulation of these key regulatory steps resulted in corneal transparency being compromised and a non-functional cornea. This is the first direct demonstration of a fundamental mechanism involving interactions of collagen I and collagen V in the regulation of collagen fibrillogenesis in tissues. Heterotypic collagen fibrils containing co-assembled collagen I and collagen V were initially described in the corneal stroma (Birk et al., 1988). It is now recognized that all fibrils are heterotypic co-assemblies of two or more fibril-forming collagens; a quantitatively major and minor collagen (Birk and Bruckner, 2011). The importance of collagen V has been suggested by studies that modulate its content in model systems, as well as EDS patients (Burrows et al., 1996; 1997; De Paepe et al., 1997; Nicholls et al., 1996; Toriello et al., 1996; Wenstrup et al., 1996; Wenstrup et al., 2006; Wenstrup et al., 2011; Bouma et al., 2001).

The cornea has served as a model for studies of collagen V function because of its high collagen V concentration (10–20%) compared with other connective tissues containing collagen I (2–5%), as well as its rigidly controlled fibrillar structure and tissue architecture, which is tightly coupled to function. To overcome the limitation of the embryonic lethality of the conventional collagen-V-knockout mice (Wenstrup et al., 2004a) and elucidate the regulatory roles of collagen V in fibrillogenesis, a conditional knockout of *Col5a1* was targeted to the corneal stroma. A mouse line where loxP elements flank exons 3 and 4 of the *Col5a1* allele was developed. Compared with wild-type mice, $Col5a1^{flox/flox}$ mice had no differences in collagen V expression or in gross and microscope phenotype, indicating that the genetic modifications had no effect on the function of the *Col5a1* allele. The conditional mouse model was used to generate a mouse line that is null for collagen V in the corneal stroma using a *Kera*-Cre mouse line that targets Cre expression to corneal keratocytes (Weng et al., 2008) and our data demonstrated stroma-specific Cre expression with no Cre activity observed in the corneal epithelium, endothelium, sclera or muscle. Breeding these $Col5a1^{flox/flox}$ mice with the Cre-expressing mouse line results in bitransgenic mice where exons 3–4 of the *Col5a1* gene are excised in stromal keratocytes. These $Col5a1^{\Delta st/\Delta st}$ mice were collagen V null and developed cloudy corneas associated with altered fibrillogenesis. This is the only known mouse model where collagen-V-knockout tissues can be analyzed in mature mice, thus allowing an analysis of its roles in the regulation of fibrillogenesis in tissues and developing organ systems. In addition, the $Col5a1^{flox/flox}$ conditional knockout mouse model allows the analysis of tissue-specific functions of collagen V by targeting Cre expression to different tissues. It also can be used to

study the function of collagen V at different times in the lifecycle of the mouse or post injury, using drug-inducible Cre-expressing mice (Chen et al., 2004).

Collagen V nucleates fibril assembly to control fibril number and initial diameter. Our data demonstrated the assembly of fewer large-diameter fibrils with a heterogeneous diameter distribution in the *Col5a1*-null corneal stroma. This is in contrast to our previous work that demonstrated a virtual lack of fibril assembly in the mesenchyme of a traditional $Col5a1^{-/-}$ mouse model (Wenstrup et al., 2004a). Our interpretation is that in mesenchyme with a low collagen I concentration, collagen V is required for fibril nucleation. Collagen I can self-assemble under physiological conditions in vitro after long lag phases and at relatively high concentrations. This indicates that nucleation of fibril assembly with collagen I alone is inefficient. Nucleators such as collagen V are not required when collagen concentrations exceed relatively high critical concentrations (Birk et al., 1990; Birk, 2001). In the current work, fibril assembly occurred in the mature corneal stroma, but lacked corneal-specific regulation, with a narrow distribution of small-diameter fibrils with near-circular fibril profiles. Our interpretation is that in the relatively high collagen concentration environment of the stroma collagen I inefficiently self-assembles. The absence of collagen V results in dysfunctional regulation of nucleation and initial fibril assembly, resulting in the aberrant fibrils observed. In the $Col5a1^{\Delta st/\Delta st}$ stroma, there was also a decrease in the number of fibrils assembled. Our hypothesis is that the collagen V content defines the number of fibrils assembled, with a large number of nucleation sites leading to more small-diameter fibrils. Collagen V interacts with collagen I during assembly, subsequently becoming incorporated into heterotypic fibrils (Birk et al., 1990; Birk, 2001; Linsenmayer et al., 1993), thereby only functioning in one round of assembly. Therefore, normal regulation of fibril number and fibril diameter is a direct result of the ratio of collagen V to collagen I content. These data strongly support a regulatory role for collagen V in the determination of fibril number.

In normal corneal development, collagen fibrils are assembled with small diameters and do not undergo the lateral fibril growth observed in most connective tissues. The regulation of lateral growth involves small leucine-rich proteoglycans (SLRPs), such as decorin, biglycan, lumican, fibromodulin and keratocan (Chakravarti et al., 1998; Ezura et al., 2000; Jepsen et al., 2002; Liu et al., 2003; Zhang et al., 2009; Chen et al., 2010). The absence of SLRPs results in unregulated lateral fusion of fibrils giving rise to 'cauliflower' cross-sectional fibril profiles. These were not observed in the current study, and there is little observed interaction of stromal fibrils. This supports an interpretation where abnormal fibril structure is the result of dysfunctional regulation of initial assembly rather than abnormal lateral growth.

Corneal transparency also requires regular fibril packing and organization into orthogonal lamellae (Hassell and Birk, 2010) and a disruption in these parameters was observed in the *Col5a1*-null stroma. The factors regulating these steps have not been not fully elucidated. However, the interactions involving matrix molecules and the cell surface, as well as the interactions between matrix components, such as proteoglycans, have been implicated (Bredrup et al., 2005; Hassell and Birk, 2010; Zhang et al., 2009). During development, initial collagen assembly occurs in close association with the keratocyte surface (Birk and Trelstad, 1984; Birk and Bruckner, 2011). We speculate that collagen V is associated with the keratocyte surface. The NH_2-non-collagenous domain of collagen V was shown to interact with numerous matrix proteins that could generate such interactions (Symoens et al., 2010). An absence of collagen V would compromise control of assembly and deposition by dissociating these processes from their normal regulatory domain. For instance, mutations in tenascin X lead to an EDS phenotype in the presence of normal collagen V (Bristow et al., 2005; Mao et al., 2002). The mechanism might be related to the uncoupling of fibril assembly from the fibroblast surface, resulting from the absence of an indirect link to the fibroblast with the overall effect being dysregulation of collagen assembly. An absence of collagen V, resulting in dissociation of initial collagen assembly from the keratocyte surface, could impact regulation in different ways. In addition to the unregulated nucleation of assembly, less-efficient assembly of collagen I would be expected. Compartmentalizing the initial assembly steps within a micro-domain provides a mechanism whereby processes important in fibril assembly such as pro-collagen processing can be integrated under cellular control. Pro-collagen processing in the absence of collagen V requires further study. Support for this suggestion is provided by studies indicating that retention of the collagen I N-propeptide is associated with irregular fibril cross-sectional profiles in EDS and other genetic diseases, and in vitro systems with defects in processing of the NH_2-propeptide (Hulmes et al., 1989; Colige et al., 2004; Lenaers et al., 1971; Steinmann et al., 2002). This could contribute to the altered fibril structure in the absence of collagen V. Collagen V interactions with the keratocytes also permit control over positioning of newly assembled fibrils, and the disruption of stromal architecture observed in the absence of collagen V supports this suggestion.

In summary, a $Col5a1^{flox/flox}$ conditional-knockout mouse line was established in this study. This enables us to explore the function of collagen V in different tissues and different developmental stages. Breeding $Col5a1^{flox/flox}$ mice with cornea-stroma-specific Cre mice, we established a cornea-stroma-specific *Col5a1* conditional-knockout mouse model. The *Col5a1*-null stroma exhibited a severe dysfunctional regulation of fibrillogenesis. The fibril diameter was increased and the fibril lamellae structure was disorganized. This structural abnormality resulted in corneal opacification and a loss of corneal function. These data indicate a key regulatory role for collagen V in the regulation of corneal collagen fibrillogenesis and development of function.

Materials and Methods

Generation of cornea-specific $Col5a1^{\Delta st/\Delta st}$ mice

The *Col5a1* sequence obtained from the Celera mouse genomic database was used to generate a *Col5a1*-targeting construct where exons 3 and 4 of the *Col5a1* gene were flanked by loxP elements. The excision of exons 3 and 4 by Cre recombinase leads to a nonsense mutation with premature termination and only a non-functional truncated small peptide of *Col5a1* could be translated. The detailed strategy is presented in Fig. 1. Basically, the targeting vector, which includes exons 3 and 4 flanked with loxP elements, a Neo cassette flanked with FRT sequences and a thymidine kinase (tk) negative selection sequence, was linearized and electroporated into 129 Sv/J mouse ES cells. After double selection with G418 and ganciclovir, ES cells containing the targeted *Col5a1* allele were identified by Southern blot using *Sph*I and *Spe*I digestion of ES cell genomic DNA. The positive ES cells heterozygous for the allele containing the integrated homologous recombinant were injected into wild-type mouse blastocysts. The chimeric males were mated with C57 BL/6 females and created targeted ($Col5a1^{ta/wt}$) mice. Then, $Col5a1^{ta/wt}$ mice were crossed with a germline-specific Flp transgenic mouse to remove the Neo cassette and generate the heterozygous floxed *Col5a1* ($Col5a1^{flox/wt}$) mice for conditional knockout. These mice were bred to homozygosity to generate homozygous $Col5a1^{flox/flox}$ mice.

To generate cornea-stroma-specific conditional-knockout mice, female keratocyte-specific keratocan-Cre (*Kera*-Cre) transgenic mice (Weng et al., 2008) were bred with male *Col5a1*$^{flox/flox}$ mice. The resulting female *Col5a1*$^{\Delta st/wt}$ mice appeared normal and were bred with male *Col5a1*$^{flox/flox}$ mice to create *Col5a1*$^{\Delta st/\Delta st}$ mice; this avoids promiscuous excision of floxed alleles during spermatogenesis in male bitransgenic *Kera*-Cre/*Col51a1*$^{flox/wt}$ mice (Weng et al., 2008). Genotyping was performed using a REDExtract-N-Amp^{TM} Tissue PCR Kit (Sigma). The primers for *Col5a1* genotyping were: Col5a1-F, TGGGATAGAGACAGGGCTTTG; Col-5a1-R, AGTCATTTGGTTCCCTCCCAG; and NeoR, ATCGCCTTCTTGACG-AGTTC. The sizes of the *Col5a1* floxed allele and wild-type allele are 272 bp and 150 bp, respectively. The primers for *Kera*-Cre are ra47, GCAGAACCTGAAGA-TGTTCGC and ra48, ACACCAGAGACGGAAATCCATC. To determine whether *Cre*-recombinase could use the inserted loxP sites to delete *Col5a1* exons 3 and 4, primers from intron 2 (TAGCCTTTGATGCAGCTGGAGACT) and intron 3 (GCCCCTTCTCTGTTTTCTGCTC) were used to verify the excision of loxP sites by Cre recombinase in the mouse cornea stroma genomic DNA. The size of the excised allele is 391 bp.

RNA isolation and quantification of mRNA

Cornea was dissected from the mice at 6 weeks and was treated with Dispase II (Roche) to separate the cornea epithelia from the cornea stroma. The stroma of cornea was cut into small pieces and total RNA from cornea stroma and epithelia was extracted using the micro RNeasy Kit (QIAGEN). 4 ng total RNA per well was subjected to reverse transcription by using the High Capacity cDNA Reverse Transcription Kit (Applied Biosystems) and the real-time PCR was performed with SYBR Green PCR master mix (Applied Biosystems) on a StepOnePlus Real Time PCR system (Applied Biosystems). The primer sequences were as follows: *Col5a1* forward primer, AAGCGTGGGAAACTGCTCTCCTAT and *Col5a1* reverse primer, AGCAGTTGTAGGTGACGTTCTGGT; actin forward primer, AGATGA-CCCAGATCATGTTTGAGA and actin reverse primer, CACAGCCTGGA-TGGCTACGT. Each sample was run in triplicate and data were analyzed using StepOne software (Applied Biosystems). Actin was used as an internal control to standardize the amount of sample total RNA.

Laser-capture microdissection was used to dissect anterior cornea stroma and posterior cornea stroma. The detailed procedure followed the Arcturus protocol. Briefly, P30 mouse eyeballs from control *Col5a1*$^{flox/flox}$ mice and *Col5a1*$^{\Delta st/\Delta st}$ mice were dissected, snap frozen, serially sectioned onto PEN membrane glass slides (Arcturus). After 70% ethanol fixation, staining and dehydration, laser-capture microdissection was performed to separately collect anterior and posterior cornea stroma samples with the Arcturus XT^{TM} system and software. The total RNA isolation was performed using the PicoPure RNA Isolation Kit (Arcturus) and the reverse transcription and real time PCR was performed as described above. The CT value was adjusted by the amplification efficiencies for each sample. Amplification efficiencies were measured by the default fit option of LinRegPCR while maintaining the cycle threshold as a data point within the measured regression line (Mienaltowski et al., 2008; Schefe et al., 2006).

Immunoblotting

Protein extracts were prepared in extracting buffer containing 50 mM Tris-HCl, pH 6.8, 1% SDS and proteinase inhibitor cocktail (Roche). 5 μg of cornea protein lysate was separated on a 4–12% Bis-Tris gel (Invitrogen) and transferred onto a Hybond-C membrane (GE Healthcare). The membrane was hybridized with anti-α1(V) antisera (Wenstrup et al., 2004a), which targeted a peptide sequence in exon 6, downstream from the exon 3–4 region targeted by homologous recombination DNA. Actin was used as a protein loading control. Actin antibody was purchased from Millipore (Billerica, MA).

Immunofluorescence microscopy

Immunofluorescence staining of collagen V in frozen sections was done in P30 mice corneas. The whole eye was fixed in fixative containing 4% paraformaldehyde, embedded in OCT medium and frozen at −80℃. Frozen sections were cut at 5 μm using a HM 505E cryostat. Before immunostaining for collagen V, the sections were pretreated with testicular hyaluronidase. Anti-mouse collagen V antibody was used at 1:400. The secondary antibody was goat anti-rabbit IgG conjugated to Alexa Fluor 568 (Invitrogen) at 1:400. Vectashield mounting solution with DAPI (Vector Laboratories, Burlingame, CA) was used as a nuclear marker. Images were captured with a Leica CTR 5500 fluorescent microscope (Wetzlar, Germany) and Leica DFC 340 FX digital camera. Antibody incubations and image acquisition were done concurrently for control *Col5a1*$^{flox/flox}$ mice and *Col5a1*$^{\Delta st/\Delta st}$ mice sections, using identical procedures and settings to facilitate comparison.

To examine the specificity and efficiency of Cre excision, female *Kera*-Cre mice were bred with mT/mG reporter male mice, which were purchased from Jackson Labs. mT/mG mouse is a dual-fluorescent Cre-reporter mouse that normally expresses membrane-bound Tomato Red (mT) fluorescence protein prior to Cre-mediated excision that leads to consequent expression of membrane-bound EGFP (Muzumdar et al., 2007). Tissues were dissected at P30, embedded in OCT and 6 μm frozen sections were cut. Fluorescence images were taken using with a Leica CTR 5500 fluorescence microscope.

Transmission electron microscopy

The corneas from *Col5a1*$^{\Delta st/\Delta st}$ and control *Col5a1*$^{flox/flox}$ mice at age P30 were used for ultrastructural analysis. The samples were prepared for transmission electron microscopy as previously described (Ansorge et al., 2009). Sections were examined and photographed at 80 kV using a JEOL 1400 transmission electron microscope with a Gatan Orius widefield side-mount digital camera.

Fibril diameter and inter fibril space measurement

Fibril diameter analysis was done as previously described (Chen et al., 2010). For the measurement of collagen fibril diameters in control mice and Col5a1 conditional-knockout mice, corneas from three different P30 mice from each phenotype were analyzed. Four non-overlapping cross-sectioned digital images were taken at 100,000× from the anterior stroma and posterior stroma of the central cornea of each specimen. Diameters were measured along the minor axis of cross-sections using an R&M Biometrics-Bioquant Image Analysis System (Nashville, TN). Data analysis and histogram were done with Microsoft Excel software. The same images were used to measure the inter-fibril space. Four non-overlapping regions of interest (ROI) from each digital image were converted to binary images, the noise outliers were removed, and then the inter-fibril area fraction was measured with ImageJ software (National Institutes of Health).

Analysis of cornea stromal haze and thickness

In vivo analysis of cornea stromal thickness and haze was performed in P60 mice under anesthesia using an in vivo confocal microscope (Heidelberg Retinal Tomograph – HRT II Rostock Cornea Module, Heidelberg Engineering, Germany) as described (Liu et al., 2010). Briefly, a drop of GenTeal Gel (Novartis Pharmaceuticals) was applied to the tip of the HRT II objective as lubricants. Subsequently, a series of images was collected from the central corneal region. A continuous *z*-axis scan was obtained through the entire cornea at 1–3 μm increments starting in front of the epithelium and ending below the endothelium. To generate depth intensity profiles, the pixel intensity in the central region (ROI) of each consecutive image was measured. The total haze of the corneal stroma was obtained by summing the pixel intensity of the ROI in the continuous planes between the subbasal epithelium and the anterior of the endothelium cells. The axial distance between these two planes represented the cornea stroma thickness. The images along the *x*–*z* planes were also used to determine the corneal stroma thickness. 3D images were reconstructed using AxioVision Imaging software.

Detection of corneal polarization by SHG imaging

Confocal imaging of second harmonic-generated (SHG) signals was used to analyze the orientation of collagen fibrils within the stroma. The detailed procedure was described previously (Liu et al., 2010; Morishige et al., 2006).

Acknowledgements

We would like to acknowledge many helpful discussions with Yayoi Izu-Takahashi. The expert technical assistance of Qingmei (Chris) Yao also is gratefully acknowledged.

Funding

This study was supported by the National Institutes of Health [grant numbers EY05129 and AR44755] (to D.E.B.) and National Institutes of Health [grant number EY011845]; Research to Prevent Blindness, Inc.; and Ohio Lions Eye Research Foundation (to W.W.K.). Deposited in PMC for release after 12 months.

References

Ansorge, H. L., Meng, X., Zhang, G., Veit, G., Sun, M., Klement, J. F., Beason, D. P., Soslowsky, L. J., Koch, M. and Birk, D. E. (2009). Type XIV collagen regulates fibrillogenesis: premature collagen fibril growth and tissue dysfunction in null mice. *J. Biol. Chem.* **284**, 8427-8438.

Beighton, P. (1992). The Ehlers-Danlos Syndromes. In *McKusick's Heritable Disorders of Connective Tissue*, (ed. P. Beighton), pp. 189-251. St. Louis: Mosby.

Beighton, P., De Paepe, A., Steinmann, B., Tsipouras, P. and Wenstrup, R. J. (1998). Ehlers-Danlos syndromes: revised nosology, Villefranche, 1997. Ehlers- Danlos National Foundation (USA) and Ehlers-Danlos Support Group (UK). *Am. J. Med. Genet.* **77**, 31-37.

Birk, D. and Bruckner, P. (2011). Collagens, suprastructures and collagen fibril assembly. In *The Extracellular Matrix: an Overview*, Vol. 1 (ed. R. P. Mecham), pp. 77-115. New York: Springer.

Birk, D. E. (2001). Type V collagen: heterotypic type I/V collagen interactions in the regulation of fibril assembly. *Micron* **32**, 223-237.

Birk, D. E. and Trelstad, R. L. (1984). Extracellular compartments in matrix morphogenesis: collagen fibril, bundle, and lamellar formation by corneal fibroblasts. *J. Cell Biol.* **99**, 2024-2033.

Birk, D. E., Fitch, J. M., Babiarz, J. P. and Linsenmayer, T. F. (1988). Collagen type I and type V are present in the same fibril in the avian corneal stroma. *J. Cell Biol.* **106**, 999-1008.

Birk, D. E., Fitch, J. M., Babiarz, J. P., Doane, K. J. and Linsenmayer, T. F. (1990). Collagen fibrillogenesis in vitro: interaction of types I and V collagen regulates fibril diameter. *J. Cell Sci.* **95**, 649-657.

Bouma, P., Cabral, W. A., Cole, W. G. and Marini, J. C. (2001). COL5A1 exon 14 splice acceptor mutation causes a functional null allele, haploinsufficiency of alpha 1(V) and abnormal heterotypic interstitial fibrils in Ehlers-Danlos syndrome II. *J. Biol. Chem.* **276**, 13356-13364.

Bredrup, C., Knappskog, P. M., Majewski, J., Rodahl, E. and Boman, H. (2005). Congenital stromal dystrophy of the cornea caused by a mutation in the decorin gene. *Invest. Ophthalmol. Vis. Sci.* **46**, 420-426.

Bristow, J., Carey, W., Egging, D. and Schalkwijk, J. (2005). Tenascin-X, collagen, elastin, and the Ehlers-Danlos syndrome. *Am. J. Med. Genet. C Semin. Med. Genet.* **139C**, 24-30.

Burrows, N. P., Nicholls, A. C., Yates, J. R., Gatward, G., Sarathachandra, P., Richards, A. and Pope, F. M. (1996). The gene encoding collagen alpha1(V)(COL5A1) is linked to mixed Ehlers-Danlos syndrome type I/II. *J. Invest. Dermatol.* **106**, 1273-1276.

Burrows, N. P., Nicholls, A. C., Yates, J. R., Richards, A. J. and Pope, F. M. (1997). Genetic linkage to the collagen alpha 1 (V) gene (COL5A1) in two British Ehlers-Danlos syndrome families with variable type I and II phenotypes. *Clin. Exp. Dermatol.* **22**, 174-176.

Chakravarti, S., Magnuson, T., Lass, J. H., Jepsen, K. J., LaMantia, C. and Carroll, H. (1998). Lumican regulates collagen fibril assembly: skin fragility and corneal opacity in the absence of lumican. *J. Cell Biol.* **141**, 1277-1286.

Chen, S., Oldberg, A., Chakravarti, S. and Birk, D. E. (2010). Fibromodulin regulates collagen fibrillogenesis during peripheral corneal development. *Dev. Dyn.* **239**, 844-854.

Chen, Y. T., Liu, P. and Bradley, A. (2004). Inducible gene trapping with drug-selectable markers and Cre/loxP to identify developmentally regulated genes. *Mol. Cell. Biol.* **24**, 9930-9941.

Colige, A., Nuytinck, L., Hausser, I., van Essen, A. J., Thiry, M., Herens, C., Ades, L. C., Malfait, F., Paepe, A. D., Franck, P. et al. (2004). Novel types of mutation responsible for the dermatosparactic type of Ehlers-Danlos syndrome (Type VIIC) and common polymorphisms in the ADAMTS2 gene. *J. Invest. Dermatol.* **123**, 656-663.

De Paepe, A., Nuytinck, L., Hausser, I., Anton-Lamprecht, I. and Naeyaert, J.-M. (1997). Mutations in the COL5A1 gene are causal in the Ehlers-Danlos syndromes I and II. *Am. J. Hum. Genet.* **60**, 547-554.

Ezura, Y., Chakravarti, S., Oldberg, A., Chervoneva, I. and Birk, D. E. (2000). Differential expression of lumican and fibromodulin regulate collagen fibrillogenesis in developing mouse tendons. *J. Cell Biol.* **151**, 779-788.

Han, M., Giese, G. and Bille, J. (2005). Second harmonic generation imaging of collagen fibrils in cornea and sclera. *Opt. Express* **13**, 5791-5797.

Hassell, J. R. and Birk, D. E. (2010). The molecular basis of corneal transparency. *Exp. Eye Res.* **91**, 326-335.

Hausser, I. and Anton-Lamprecht, I. (1994). Differential ultrastructural aberrations of collagen fibrils in Ehlers-Danlos syndrome types I-IV as a means of diagnostics and classification. *Hum. Genet.* **93**, 394-407.

Hulmes, D. J., Kadler, K. E., Mould, A. P., Hojima, Y., Holmes, D. F., Cummings, C., Chapman, J. A. and Prockop, D. J. (1989). Pleomorphism in type I collagen fibrils produced by persistence of the procollagen N-propeptide. *J. Mol. Biol.* **210**, 337-345.

Jepsen, K. J., Wu, F., Peragallo, J. H., Paul, J., Roberts, L., Ezura, Y., Oldberg, A., Birk, D. E. and Chakravarti, S. (2002). A syndrome of joint laxity and impaired tendon integrity in lumican- and fibromodulin-deficient mice. *J. Biol. Chem.* **277**, 35532-35540.

Lenaers, A., Ansay, M., Nusgens, B. V. and Lapiere, C. M. (1971). Collagen made of extended α-chains, procollagen, in genetically-defective dermatosparaxic calves. *Eur. J. Biochem.* **23**, 533-543.

Linsenmayer, T. F., Gibney, E., Igoe, F., Gordon, M. K., Fitch, J. M., Fessler, L. I. and Birk, D. E. (1993). Type V collagen: molecular structure and fibrillar organization of the chicken alpha 1(V) NH2-terminal domain, a putative regulator of corneal fibrillogenesis. *J. Cell Biol.* **121**, 1181-1189.

Liu, C. Y., Birk, D. E., Hassell, J. R., Kane, B. and Kao, W. W. (2003). Keratocan-deficient mice display alterations in corneal structure. *J. Biol. Chem.* **278**, 21672-21677.

Liu, H., Zhang, J., Liu, C. Y., Wang, I. J., Sieber, M., Chang, J., Jester, J. V. and Kao, W. W. (2010). Cell therapy of congenital corneal diseases with umbilical mesenchymal stem cells: lumican null mice. *PLoS ONE* **5**, e10707.

Malfait, F., Wenstrup, R. J. and De Paepe, A. (2010). Clinical and genetic aspects of Ehlers-Danlos syndrome, classic type. *Genet. Med.* **12**, 597-605.

Mao, J. R., Taylor, G., Dean, W. B., Wagner, D. R., Afzal, V., Lotz, J. C., Rubin, E. M. and Bristow, J. (2002). Tenascin-X deficiency mimics Ehlers-Danlos syndrome in mice through alteration of collagen deposition. *Nat. Genet.* **30**, 421-425.

Marchant, J. K., Hahn, R. A., Linsenmayer, T. F. and Birk, D. E. (1996). Reduction of type V collagen using a dominant-negative strategy alters the regulation of fibrillogenesis and results in the loss of corneal-specific fibril morphology. *J. Cell Biol.* **135**, 1415-1426.

Mienaltowski, M. J., Huang, L., Stromberg, A. J. and MacLeod, J. N. (2008). Differential gene expression associated with postnatal equine articular cartilage maturation. *BMC Musculoskelet. Disord.* **9**, 149.

Morishige, N., Petroll, W. M., Nishida, T., Kenney, M. C. and Jester, J. V. (2006). Noninvasive corneal stromal collagen imaging using two-photon-generated second-harmonic signals. *J. Cataract Refract. Surg.* **32**, 1784-1791.

Muzumdar, M. D., Tasic, B., Miyamichi, K., Li, L. and Luo, L. (2007). A global double-fluorescent Cre reporter mouse. *Genesis* **45**, 593-605.

Nicholls, A. C., Oliver, J. E., McCarron, S., Harrison, J. B., Greenspan, D. S. and Pope, F. M. (1996). An exon skipping mutation of a type V collagen gene (COL5A1) in Ehlers-Danlos syndrome. *J. Med. Genet.* **33**, 940-946.

Schefe, J. H., Lehmann, K. E., Buschmann, I. R., Unger, T. and Funke-Kaiser, H. (2006). Quantitative real-time RT-PCR data analysis: current concepts and the novel "gene expression's CT difference" formula. *J. Mol. Med.* **84**, 901-910.

Schwarze, U., Atkinson, M., Hoffman, G. G., Greenspan, D. S. and Byers, P. H. (2000). Null alleles of the COL5A1 gene of type V collagen are a cause of the classical forms of Ehlers-Danlos syndrome (types I and II). *Am. J. Hum. Genet.* **66**, 1757-1765.

Segev, F., Heon, E., Cole, W. G., Wenstrup, R. J., Young, F., Slomovic, A. R., Rootman, D. S., Whitaker-Menezes, D., Chervoneva, I. and Birk, D. E. (2006). Structural abnormalities of the cornea and lid resulting from collagen V mutations. *Invest. Ophthalmol. Vis. Sci.* **47**, 565-573.

Steinmann, B., Royce, P. M., Superti-Furga, A. (2002). The Ehlers-Danlos Syndrome. In *Connective Tissue and Its Heritable Disorders*, (ed. P. Royce, B. Steinman), pp. 431-523. New YorkNY: Wiley-Liss, Inc.

Symoens, S., Renard, M., Bonod-Bidaud, C., Syx, D., Vaganay, E., Malfait, F., Ricard-Blum, S., Kessler, E., Van Laer, L., Coucke, P. et al. (2010). Identification of binding partners interacting with the alpha1-N-propeptide of type V collagen. *Biochem. J.* **433**, 371-381.

Toriello, H. V., Glover, T. W., Takahara, K., Byers, P. H., Miller, D. E., Higgins, J. V. and Greenspan, D. S. (1996). A translocation interrupts the COL5A1 gene in a patient with Ehlers-Danlos syndrome and hypomelanosis of Ito. *Nat. Genet.* **13**, 361-365.

Vogel, A., Holbrook, K. A., Steinmann, B., Gitzelmann, R. and Byers, P. H. (1979). Abnormal collagen fibril structure in the gravis form (type I) of Ehlers-Danlos syndrome. *Laboratory Investigation* **40**, 201-206.

Weng, D. Y., Zhang, Y., Hayashi, Y., Kuan, C. Y., Liu, C. Y., Babcock, G., Weng, W. L., Schwemberger, S. and Kao, W. W. (2008). Promiscuous recombination of LoxP alleles during gametogenesis in cornea Cre driver mice. *Mol. Vis.* **14**, 562-571.

Wenstrup, R. J., Langland, G. T., Willing, M. C., D'Souza, V. N. and Cole, W. G. (1996). A splice-junction mutation in the region of proa1(V) chains results in the gravis formof the Ehlers-Danlos syndrome (type I). *Hum. Mol. Genet.* **5**, 1733-1736.

Wenstrup, R. J., Florer, J. B., Willing, M. C., Giunta, C., Steinmann, B., Young, F., Susic, M. and Cole, W. G. (2000). COL5A1 haploinsufficiency is a common molecular mechanism underlying the classical form of EDS. *Am. J. Hum. Genet.* **66**, 1766-1776.

Wenstrup, R. J., Florer, J. B., Brunskill, E. W., Bell, S. M., Chervoneva, I. and Birk, D. E. (2004a). Type V collagen controls the initiation of collagen fibril assembly. *J. Biol. Chem.* **279**, 53331-53337.

Wenstrup, R. J., Florer, J. B., Cole, W. G., Willing, M. C. and Birk, D. E. (2004b). Reduced type I collagen utilization: a pathogenic mechanism in COL5A1 haplo-insufficient Ehlers-Danlos syndrome. *J. Cell Biochem.* **92**, 113-124.

Wenstrup, R. J., Florer, J. B., Davidson, J. M., Phillips, C. L., Pfeiffer, B. J., Menezes, D. W., Chervoneva, I. and Birk, D. E. (2006). Murine model of the Ehlers-Danlos syndrome. col5a1 haploinsufficiency disrupts collagen fibril assembly at multiple stages. *J. Biol. Chem.* **281**, 12888-12895.

Wenstrup, R. J., Smith, S. M., Florer, J. B., Zhang, G., Beason, D. P., Seegmiller, R. E., Soslowsky, L. J. and Birk, D. E. (2011). Regulation of collagen fibril nucleation and initial fibril assembly involves coordinate interactions with collagens V and XI in developing tendon. *J. Biol. Chem.* **286**, 20455-20465.

Zhang, G., Chen, S., Goldoni, S., Calder, B. W., Simpson, H. C., Owens, R. T., McQuillan, D. J., Young, M. F., Iozzo, R. V. and Birk, D. E. (2009). Genetic evidence for the coordinated regulation of collagen fibrillogenesis in the cornea by decorin and biglycan. *J. Biol. Chem.* **284**, 8888-8897.